

## Supplementary Materials for

### Flexible graphene photodetectors for wearable fitness monitoring

Emre O. Polat, Gabriel Mercier, Ivan Nikitskiy, Eric Puma, Teresa Galan, Shuchi Gupta, Marc Montagut, Juan José Piqueras, Maryse Bouwens, Turgut Durduran, Gerasimos Konstantatos\*, Stijn Goossens\*, Frank Koppens\*

\*Corresponding author. Email: gerasimos.konstantatos@icfo.eu (G.K.); stijn.goossens@icfo.eu (S.G.); frank.koppens@icfo.eu (F.K.)

Published 13 September 2019, *Sci. Adv.* **5**, eaaw7846 (2019)

DOI: 10.1126/sciadv.aaw7846

#### The PDF file includes:

- Fig. S1. PPG readings of GQD Health Patch under various light conditions for the same applied bias.
- Fig. S2. Flexible and transparent GQD assembly on PEN and the dynamic range of flexible GQD PDs.
- Fig. S3. Noise characteristics of flexible GQD PDs.
- Fig. S4. Gate modulation of flexible gated GQD PDs.
- Fig. S5. Photosensitivity for various operation frequencies.
- Fig. S6. Temporal response of the flexible GQD PD at 633 nm.
- Fig. S7. Photoresponse of flexible GQD PDs at near-infrared wavelength.
- Fig. S8. Continuous PPG reading by GQD health patch.
- Fig. S9. Simultaneous measurements of GQD health patch and state-of-the-art capnograph.
- Fig. S10. Large-area Raman spectroscopy mapping of graphene on flexible polymer substrates.
- Table S1. Demonstrated device types and their specifications.
- Legends for movies S1 and S2

#### Other Supplementary Material for this manuscript includes the following:

(available at [advances.sciencemag.org/cgi/content/full/5/9/eaaw7846/DC1](https://advances.sciencemag.org/cgi/content/full/5/9/eaaw7846/DC1))

Movie S1 (.mp4 format). GQD bracelet (reflection mode PPG).

Movie S2 (.mp4 format). GQD health patch on the mobile phone screen (transmission mode PPG).

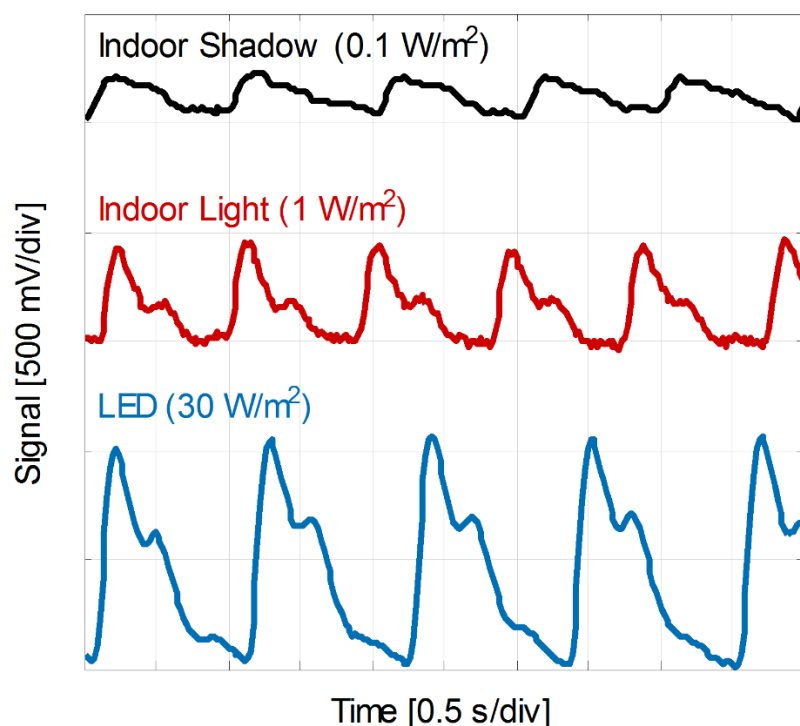


**Fig. S1.** PPG readings of GQD Health Patch under various light conditions for the same applied bias.

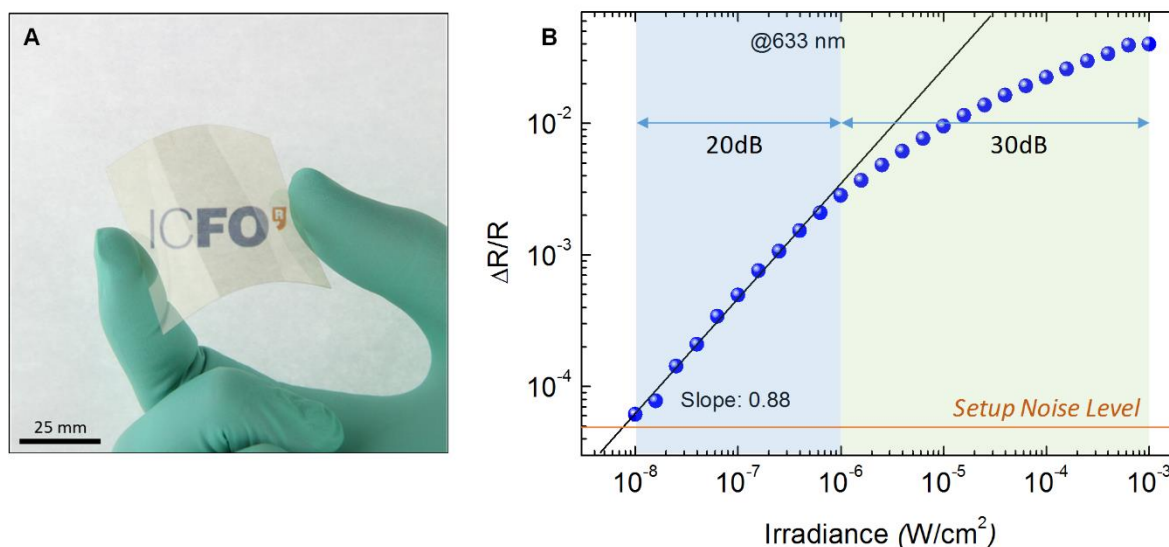


**Fig. S2.** Flexible and transparent GQD assembly on PEN and the dynamic range of flexible GQD PDs. (A), 30 nm thin film of colloidal PbS quantum dots are spin coated on single layer CVD Graphene. The background logo is clearly visible due to high transparency of the structure. (B) Photo-induced resistance change versus irradiance at 633 nm. Slope of the linear regime and high dynamic range of the detector is shown. The readout electronics limits the total dynamic range of the PDs. (Photo credit: Alina Hirschmann, ICFO-Institut de Ciències Fotoniques)

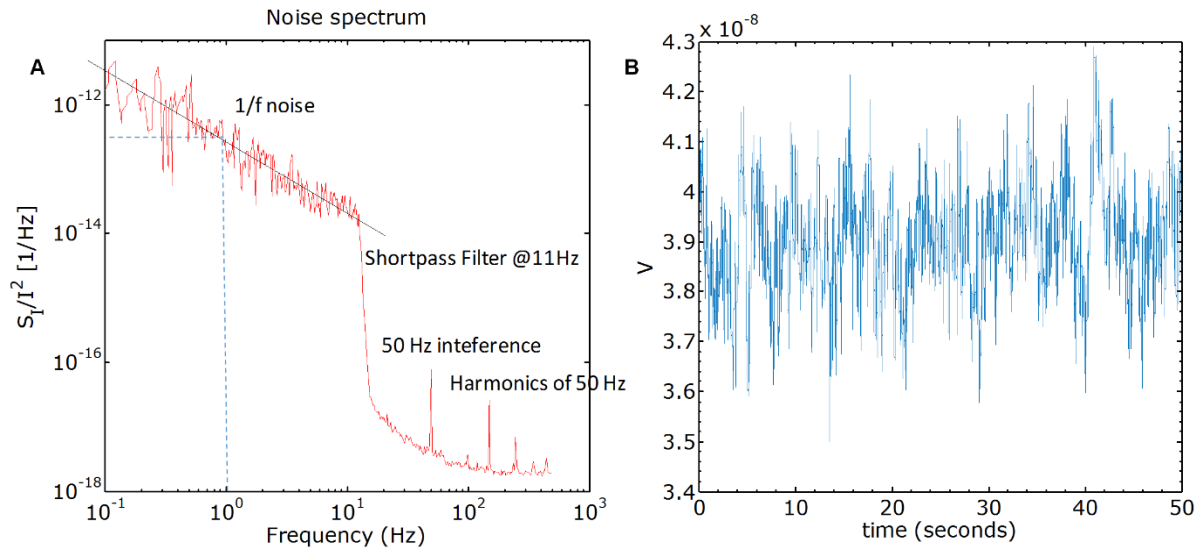


**Fig. S3. Noise characteristics of flexible GQD PDs.** (A) Noise spectral density versus frequency. Measured with 9 V battery source, by connecting the PD and 10 kOhm resistor in series. Device resistance measured to be 1.6 kOhms whereas the total current flowing through is  $7.76 \times 10^{-4}$  A.  $1/f$  noise scales inverse linearly with frequency. Device noise at 1 Hz is extracted to be around  $2 \times 10^{-13}$ . Short pass filter is AC coupled, and filters at 11 Hz to cut 50 Hz interference. (B) Time trace of the noise fluctuation.

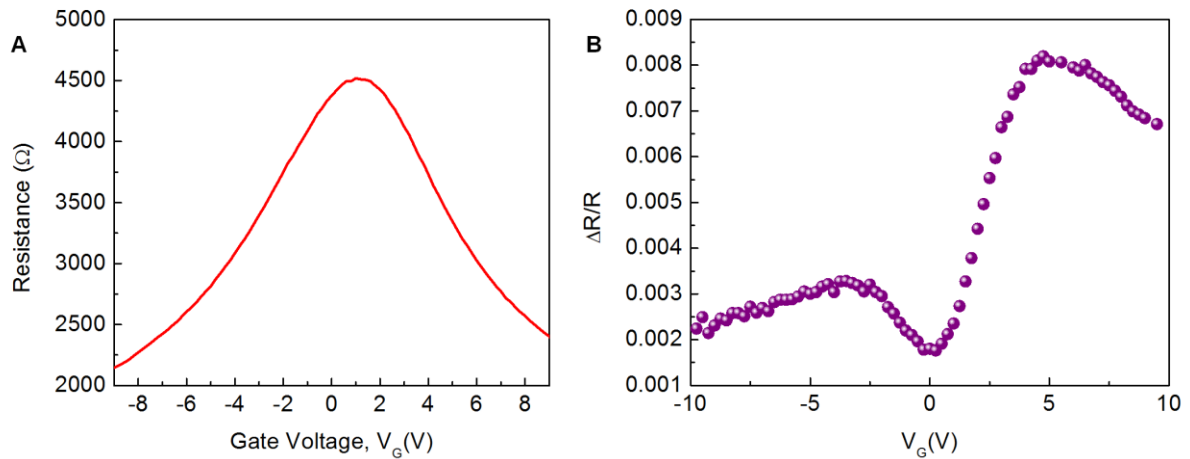


**Fig. S4. Gate modulation of flexible gated GQD PDs.** (A) Resistance vs. gate voltage sweep, for a GQD PD with a of  $50 \times 50 \mu\text{m}$  channel. Gate voltage is applied to the deposited  $50 \mu\text{m}$  Al gate, using a dielectric of  $100 \mu\text{m}$  thick  $\text{Al}_2\text{O}_3$  dielectric deposited by ALD. (B) Photo-induced resistance change versus gate voltage for the irradiance of  $0.3 \text{ W/m}^2$ , at  $633 \text{ nm}$ , with a toggling frequency of 100 Hz.

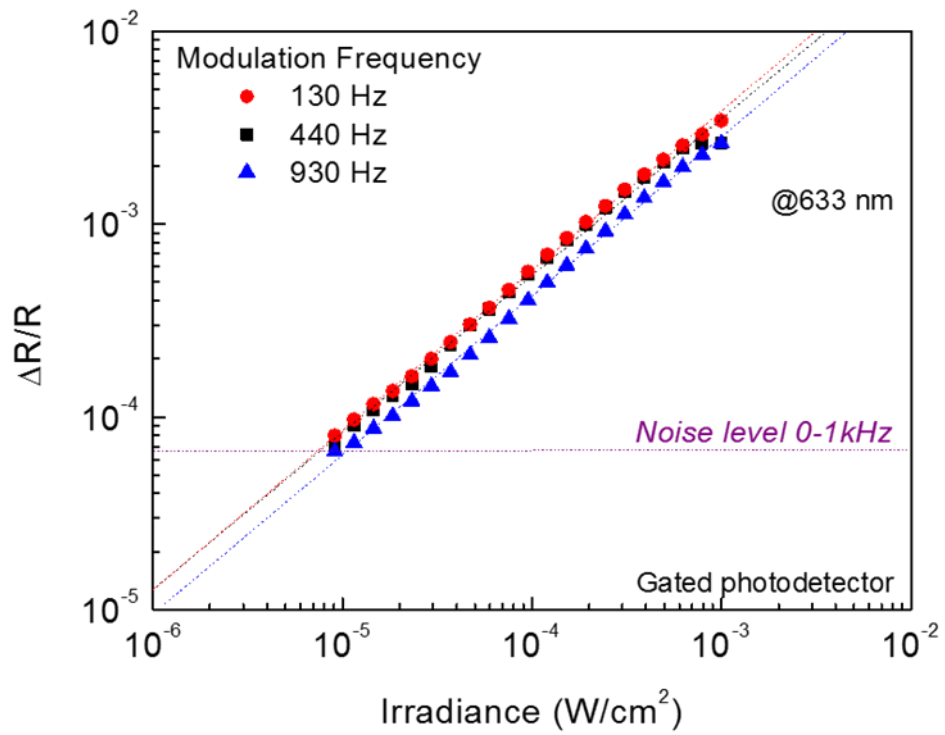


**Fig. S5. Photosensitivity for various operation frequencies.** Photo-induced resistance change versus irradiance for various frequencies. Under the application of a constant gate voltage, the PDs sustain high frequency operation. The PD sensitivity exhibits minimal change with the increasing frequency

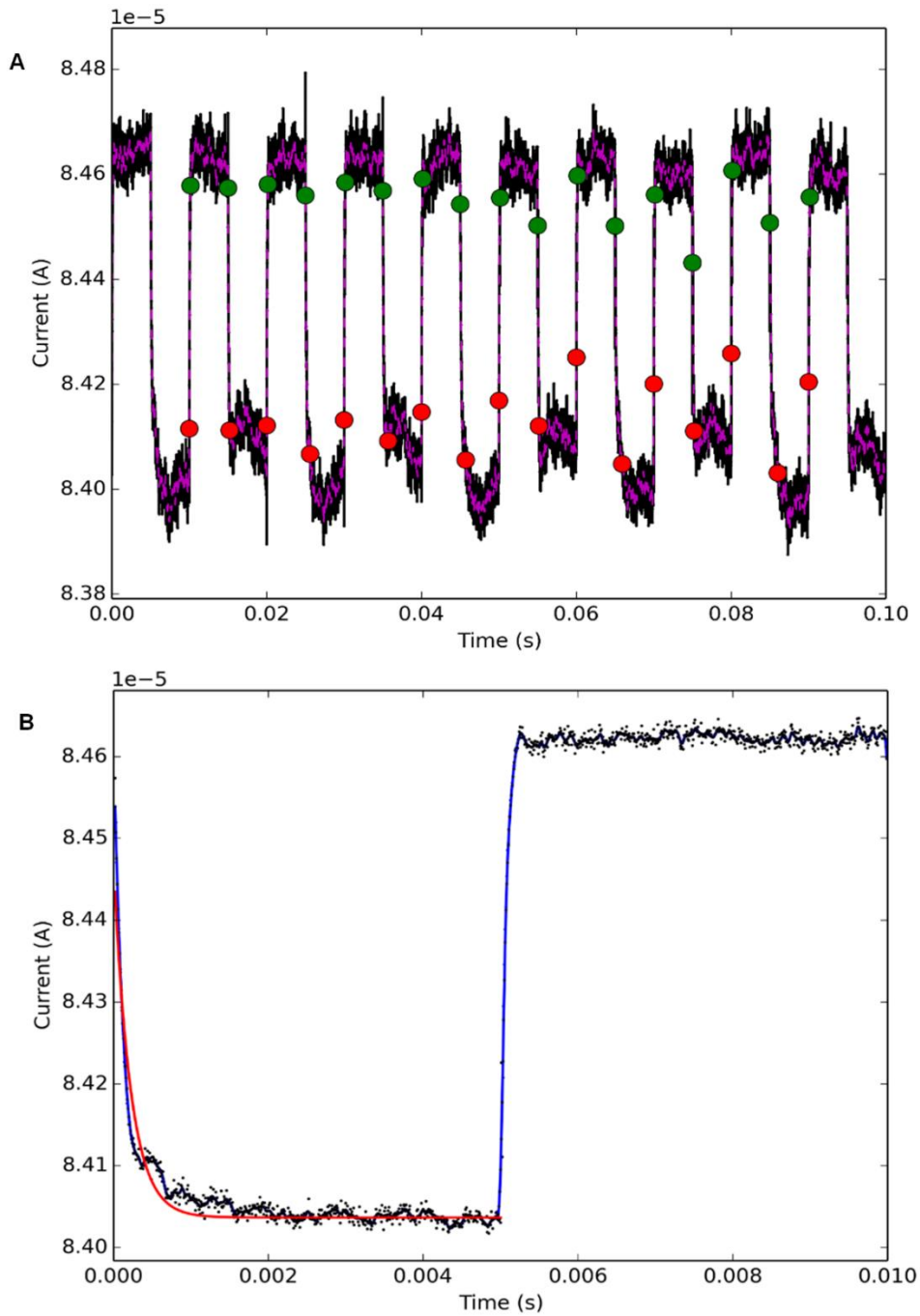


**Fig. S6. Temporal response of the flexible GQD PD at 633 nm.** (A) Photoresponse of the detector for 100 Hz light toggling. Green and red dots assigned automatically by the software showing 90% of the total photo induced current modulation to calculate  $\Delta R/R$  systematically. (B) Zoomed-in cycle of photo switching and the exponential fit during light-off response. Black dots represents the raw data points. Exponential fit yields a light-off response time around  $\tau_{\text{off}} = 200 \mu\text{s}$ , whereas light-on response time is around  $\tau_{\text{on}} = 50 \mu\text{s}$ .

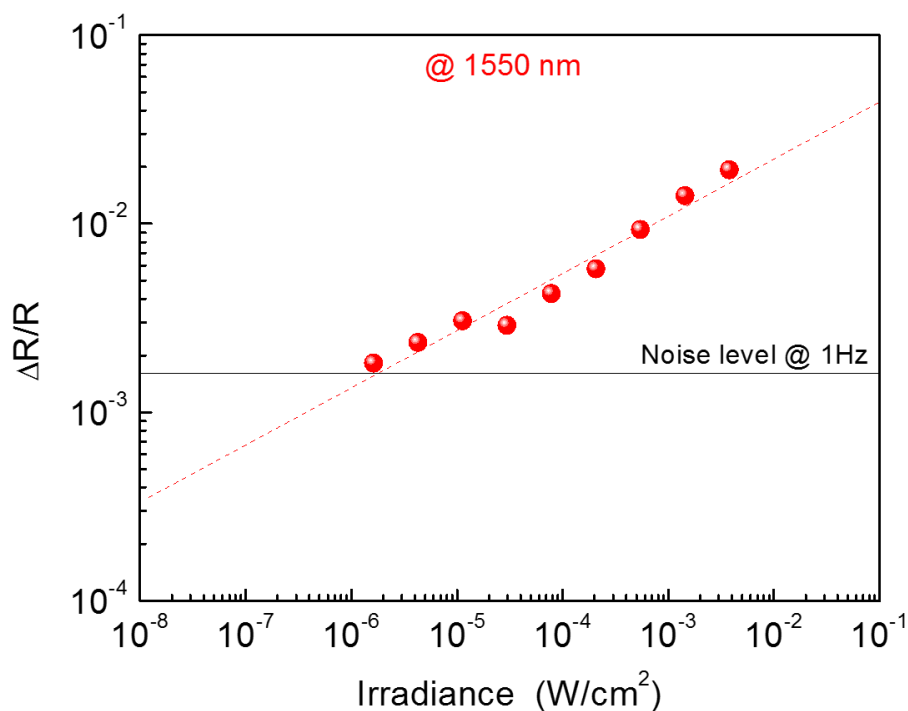


**Fig. S7. Photoresponse of flexible GQD PDs at near-infrared wavelength.** Photo-induced resistance change vs. irradiance at 1550 nm. Multiwavelength absorption of the PbS colloidal quantum dot layer allows a broadband operation from IR to UV. Similar to the visible range, the PDs exhibit a linear response in logarithmic proportions at 1550 nm, offering a linear dynamic range of around 40 dB. Infrared absorption of the deposited PbS quantum dot layer is less compared to absorption in the visible, therefore yielding a narrower total dynamic range.

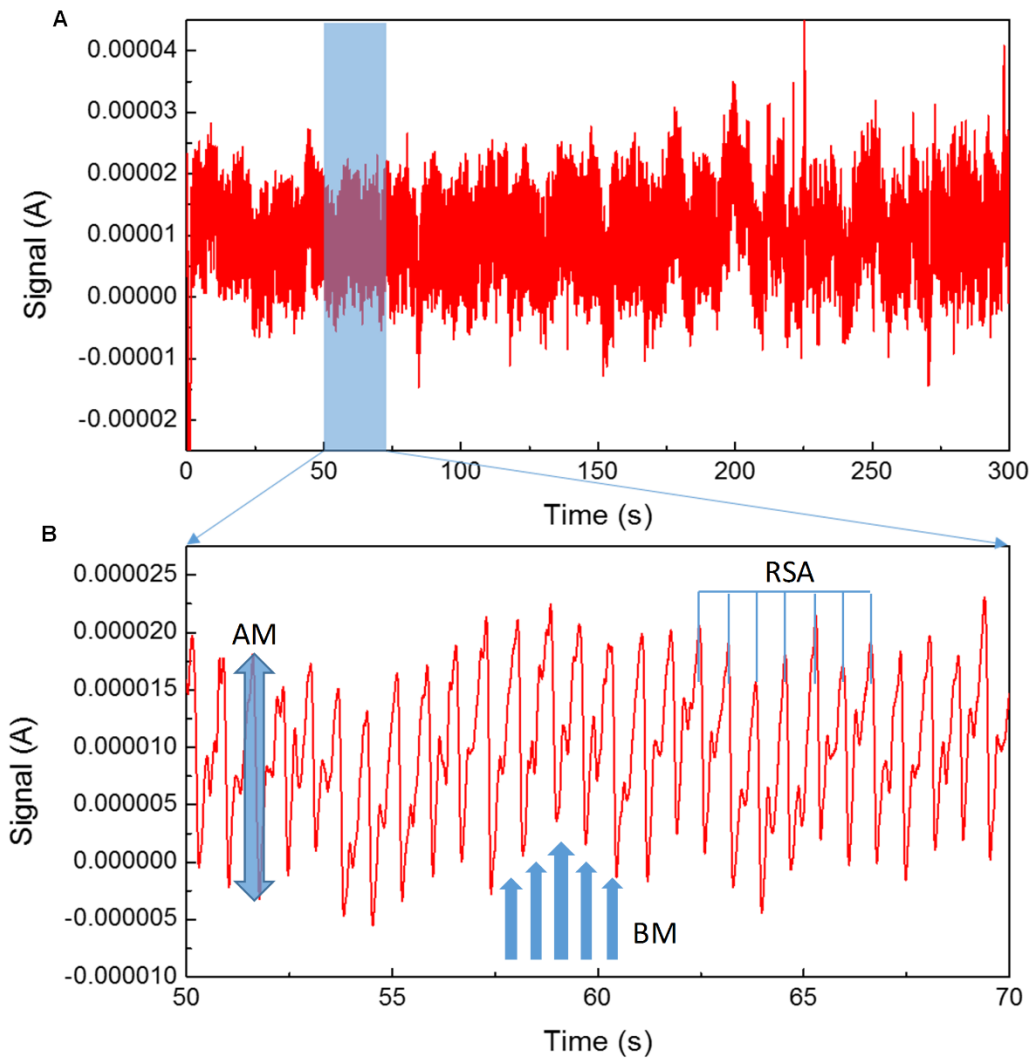


**Fig. S8. Continuous PPG reading by GQD health patch.** (A) Five minutes of transmission mode PPG reading from an individual. Measurement taken from finger using only ambient light ( $1 \text{ W/m}^2$ ). Sudden jumps in the signal amplitude around 200-250s is due to the movement of the finger. Heart rate monitoring remains unaffected from motion artifacts as long as the skin contact is preserved. (B) Zoomed in PPG reading for 20 seconds. Modulation of the AC signal due to systolic and diastolic phases of cardiac cycle can be clearly seen (AM). On the other hand, the act of respiration shows itself as a baseline DC modulation (BM) and respiratory sinus arrhythmia (RSA).

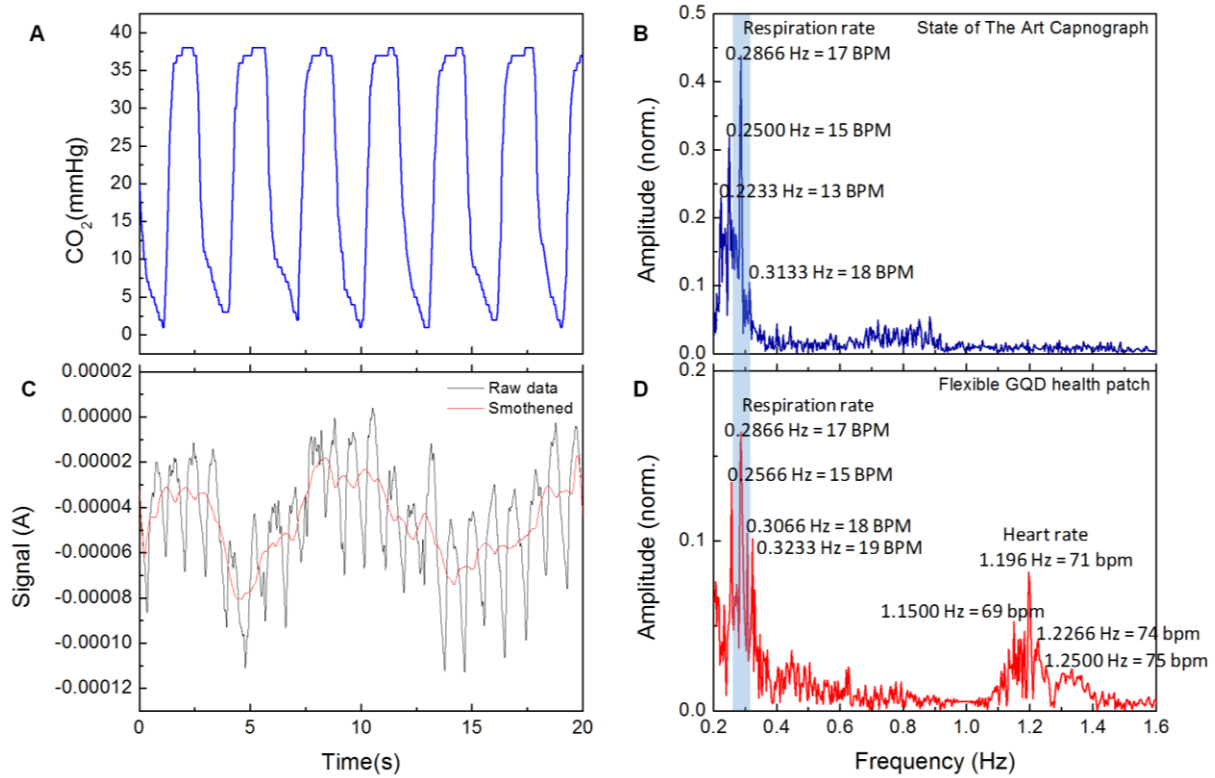


**Fig. S9. Simultaneous measurements of GQD health patch and state-of-the-art capnograph.** (A) Real time respiratory  $\text{CO}_2$  pressure cycle measured by Medtronics 20p capnograph. (B) The corresponding Fourier transform. (C) Simultaneous PPG reading from GQD health patch and the applied data smoothening to trace the effect of respiration. (D) The corresponding Fourier transform showing dynamics changes of the respiratory rate and heart rate over 5 minutes. Dominant respiration rate is extracted to be 17 breathes per minute at both methods. Harmonics around the dominant peak is observed to be at the respiration rate of 13, 15, 18, 19 breaths per minute.



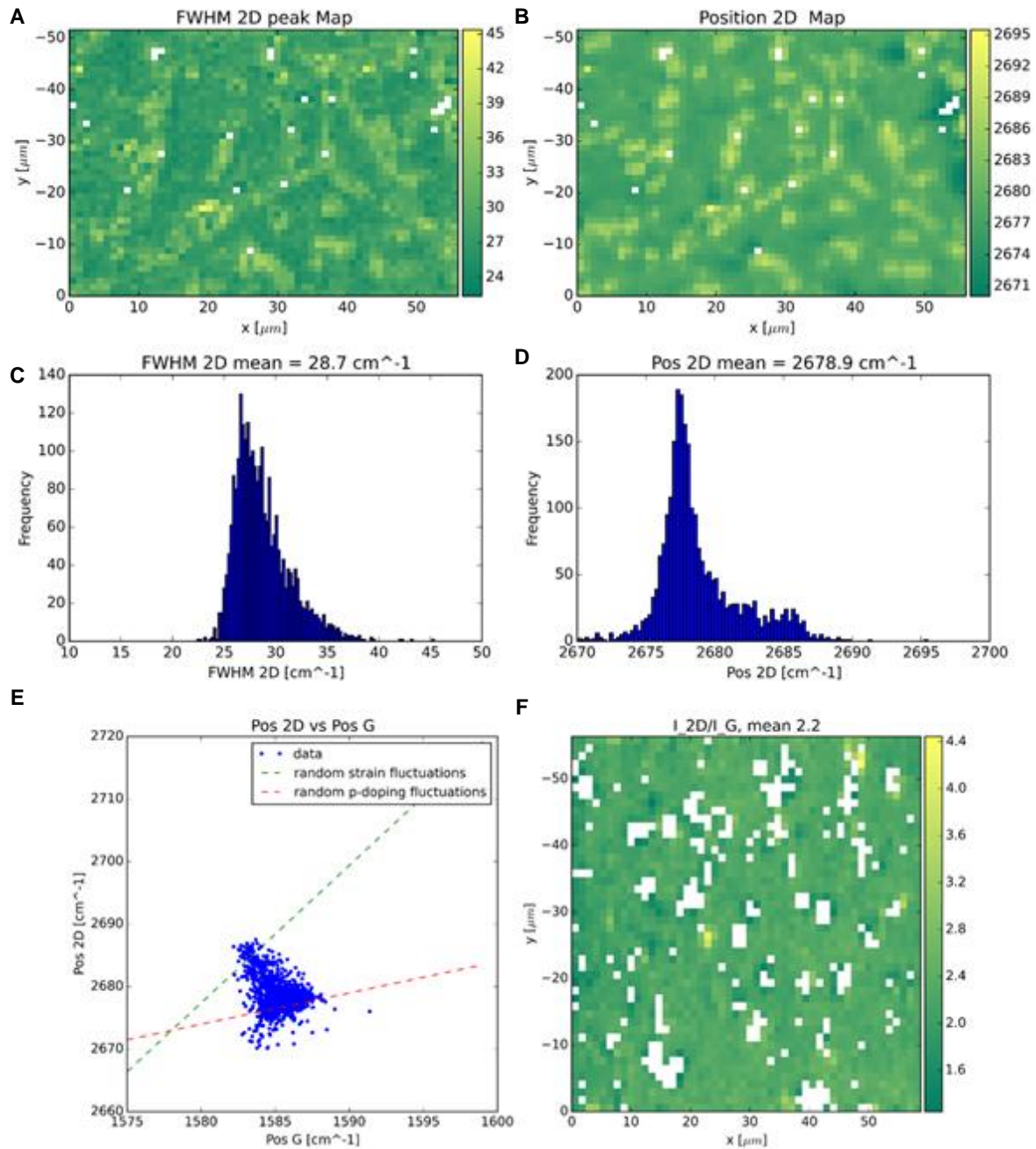


**Fig. S10. Large-area Raman spectroscopy mapping of graphene on flexible polymer substrates.** (A) Full width at half maximum (FWHM) of the Raman 2D peak mapped for  $50 \times 50 \mu\text{m}^2$  area. (B) Position map of the Raman 2D peak. (C) Histogram of the Raman 2D peak FWHM over the scanned graphene area. The scanned area contains high quality graphene with an average FWHM of  $28.7 \text{ cm}^{-1}$ . (D) Histogram of Raman 2D peak position. (E) Scatter plot of 2D peak position vs G peak position. Dashed lines represents the fluctuations in the position of both peaks due to strain and p-doping of graphene. (F) Intensity ratio map of 2D peak to G peak. Intensity of the peaks sourced from the flexible polymer substrates often dominates in the spectrum where the G peak of graphene is located. That yields indefinite points in the 2D to G peak intensity ratio map, shown as white points. We extracted an average peak intensity ratio of 2.2.

**Table S1. Demonstrated device types and their specifications.**

Device Type	Device Size	Responsivity at 633 nm (A/W)	Flexibility	Vital Signs Extracted
GQD on PEN	1 mm <sup>2</sup>	10 <sup>3</sup>	Fully Flexible	Heart Rate, Respiration Rate
Gated GQD on Polyimide	50 μm <sup>2</sup>	10 <sup>5</sup>	Limited to Dielectric Thickness	
Macroscale GQD on PET	2 cm <sup>2</sup>	5x10 <sup>2</sup>	Fully Flexible	
Integrated GQD on Thermoplastic	12 mm <sup>2</sup>	2.5x10 <sup>2</sup>	Fully Flexible	UV Skin Exposure

**Movie S1. GQD bracelet (reflection mode PPG).**

**Movie S2. GQD health patch on the mobile phone screen (transmission mode PPG).**